

***In situ* high-pressure x-ray-diffraction study of TlReO₄ to 14.5 GPa: Pressure-induced phase transformations and the equation of state**

L. C. Ming and A. Jayaraman

*Hawaii Institute of Geophysics and Planetology, School of Ocean and Earth Science & Technology,
University of Hawaii at Manoa, Honolulu, Hawaii 96822*

S. R. Shieh

*Department of Geology and Geophysics, School of Ocean and Earth Science & Technology, University of Hawaii at Manoa,
Honolulu, Hawaii 96822*

Y. H. Kim

*Department of Geology, College of Natural Sciences, Gyeongsang National University, Jinju 660-701, Korea
(Received 29 November 1994)*

In situ high-pressure x-ray-diffraction studies have been carried out on TlReO₄ up to 14.5 GPa at room temperature using a diamond-anvil cell. The x-ray data show that the orthorhombic D_{2h}^{16} TlReO₄ (I) transforms to another closely related orthorhombic phase, TlReO₄ (I') around 1.0 GPa, then to a wolframite-related monoclinic phase TlReO₄ (II) near 2.0 GPa, and finally to a BaWO₄ (II)-related monoclinic phase TlReO₄ (III) at about 10 GPa. The volume change at the first transition is negligible, and about 2% and 9%, respectively, at the two subsequent transitions. The results suggest a very minor change in structure at the first transition. The 2% ΔV at the second transition is consistent with the proposed structural arrangement from pseudoscheelite phase (I') to the wolframite phase (II). The large ΔV at the third transition is attributed to a change to a truly octahedral coordination for Re with respect to oxygens. All the three high-pressure phases of TlReO₄ are unquenchable and revert back to the low-pressure orthorhombic phase (I) on release of pressure. The results are in very good agreement with those obtained in a previous high-pressure Raman study up to 15 GPa. From pressure-volume data, we obtain a value of 26 GPa for the bulk modulus K_0 of phases (I) and (I'). The bulk moduli of phases (II) and (III) have been calculated as 45.6 and 47.6 GPa, respectively.

I. INTRODUCTION

Thallium perrhenate (TlReO₄) crystallizes in the orthorhombic pseudoscheelite structure (space group D_{2h}^{16}) under ambient conditions and is known to transform to the tetragonal scheelite structure (space group $I4_1/a$) upon heating to 400 K. Surprisingly, a similar phase change seems to occur upon cooling to 200 K.¹ A high-pressure Raman study has shown that three pressure-induced phase transitions occur at 0.5, 1.9, and 9.7 GPa, respectively, upon compression at room temperature. Jayaraman, Kourouklis, and Van Uiter² noted at the 10 GPa transition a rather striking color change in the sample, from colorless to black. For this spectacular change in the optical absorption, they have proposed an electronic transition mechanism involving a change in the valence state of Tl⁺¹ to Tl⁺³ and concurrently of Re⁺⁷ to Re⁺⁵. We felt that an x-ray-diffraction study could lead to a deeper understanding of the structural aspects of the pressure-induced phases, since Raman data alone are not adequate to arrive at the structure. We have therefore investigated TlReO₄ up to 14.5 GPa by the conventional film-method using an in-house x-ray source and also by the energy-dispersive technique using synchrotron radiation. Results of these measurements and the structures which they lead us to are presented and discussed in this paper.

II. EXPERIMENTAL METHODS

Finely powdered TlReO₄ used in this study was obtained by grinding single-crystal samples, which had been synthesized at AT&T Bell Laboratories, Murray Hill, NJ and used in the high-pressure Raman measurements reported previously.^{1,2} X-ray-diffraction analysis carried out with a Debye-Scherrer camera (57.296 mm in diameter) confirmed the orthorhombic unit cell with lattice parameters $a = 5.631(3)$ Å, $b = 5.839(2)$ Å, and $c = 13.313(15)$ Å, in good agreement with those reported by Jayaraman *et al.*¹

All high-pressure x-ray studies were carried out with a gasketed diamond-anvil cell. Both energy-dispersive x-ray diffraction with synchrotron radiation and the angular-dispersive diffraction with a conventional x-ray source were employed in the study. The energy-dispersive x-ray diffraction experiments were performed at the Stanford Synchrotron Radiation Laboratory (SSRL), and the angular-dispersive runs at the University of Hawaii. Experimental setup for these two diffraction techniques and the diamond cell have been described previously.^{3,4}

In the energy-dispersive experiments, a mixture of NaCl and finely ground sample of TlReO₄ (1:1 in volume ratio) was used, in which NaCl served both as a pressure marker and the pressure medium. Pressure was deter-

mined from the (200) and (220) peaks of NaCl along with the established equation of state of NaCl (Ref. 5) and is believed to be true to $\pm 3\%$ in the 0 to 30 GPa range. With the storage ring operating at 3 GeV and 90–60 mA, and the incident beam collimated to 50 μm in diameter, each energy spectra was collected for 5 min in real time. In our preliminary run, partly due to the limited beam-time available and partly due to the unexpected poor sample conditions at high pressures, we have only successfully obtained good quality spectra up to 3.5 GPa.

In the angular-dispersive runs, the pure sample powder together with a tiny ruby chip was used. Pressure was determined by the ruby fluorescence technique.⁴ With the x-ray generator operating at 50 kV and 26 mA and a finely collimated incident beam of Zr-filtered Mo $K\alpha$ radiation ($\sim 120\mu$), the average exposure time for each experiment was ~ 70 h.

III. RESULTS AND DISCUSSIONS

High-pressure phase transformations

In situ x-ray-diffraction data are presented in Fig. 1 showing the effect of pressure on the interplanar d spacings. Generally speaking, data obtained from two different methods are in reasonably good agreement. In determining the unit cell using the x-ray diffraction data, we have set two important criteria: (1) that the unit cell should be able to generate a set of d spacings that fit the observed diffraction data, and (2) that the molar volume

of the phase obtained from the unit cell at a given pressure is smaller than the molar volume of the preceding phase at the corresponding pressure. This procedure led to the identification of two new high-pressure phases: a monoclinic phase (II) between 2 and 7.5 GPa, and another monoclinic phase (III) above 10 GPa, in good agreement with the major phase transitions observed at 1.9 and 9.7 GPa in previous Raman-scattering study.³

Typical x-ray-diffraction data for the phases (II) and (III) are given in Tables I and II, respectively. Assuming the number of molecules per unit cell to be 4 for phases (I) and (II) and 8 for phase (III), we have obtained the lattice parameters and the molar volumes of phase (I), (II), and (III) at the given pressure. The results are presented in Table III and are plotted in Figs. 2 and 3 against pressure for the lattice parameters and the molar volume, respectively. The volume discontinuities at the transitions can be seen in Fig. 3, and these correspond to a ΔV of $\sim 2\%$ for phase (I)-phase (II) transition near 2.0 GPa and $\sim 9\%$ for phase (II)-phase (III) transition near 10 GPa.

TiReO₄ (I')

The lattice parameters of the orthorhombic phase (I) behave anomalously near 0.8 GPa (see Fig. 2). Near 1.0 GPa, while the b axis appears to follow the trend smoothly, the a axis decreases abruptly by 1.6% and the c axis increases by 1.1%. At pressures above 1.0 GPa, both a and c axes decrease smoothly with pressure, while the b axis increases. The above anomalous behavior suggests strongly the presence of a new high-pressure phase above 1.0 GPa. The structure change involved must be subtle because the diffraction lines observed in both phases are

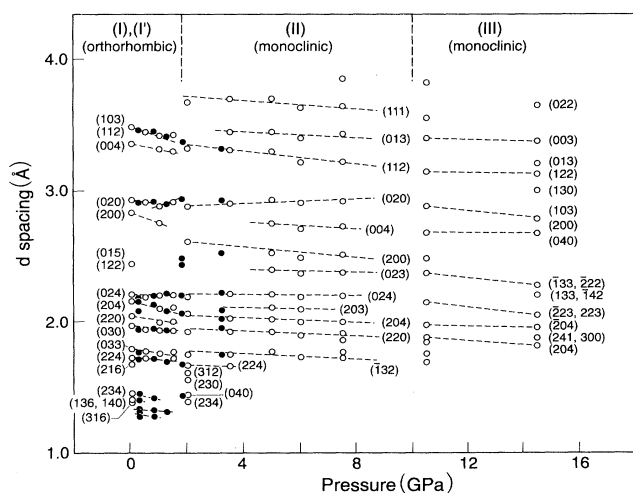


FIG. 1. Effect of pressure on the interplanar d spacings in TiReO₄ (I), (I'), (II), and (III). Open circles represent the angular-dispersive runs and solid circles the energy-dispersive runs. The (hkl) Miller indices are given on the right side for phases (II) and (III) and on the left side for (I)-(I'). The diffraction pattern assigned to phase (III) at the 10.5 GPa is a mixed phase, as revealed by diffraction lines belonging to phase (II).

TABLE I. X-ray-diffraction data of TiReO₄ (II) at 2.0 GPa and at room temperature.

I/I_0	$d_{(\text{obs})}$	(hkl)	$d_{(\text{cal})}^a$
10	3.673	(111)	3.698
100	3.320	($\bar{1}$ 12)	3.337
		(004)	3.320
50	2.868	(014)	2.874
		(020)	2.870
25	2.597	(200)	2.600
40	2.181	(024)	2.171
15	2.044	(204)	2.050
		($\bar{1}$ 06)	2.039
40	1.914	(220)	1.927
		(030)	1.913
		(221)	1.908
40	1.735	($\bar{1}$ 32)	1.734
20	1.660	(224)	1.668
10	1.610	(303)	1.616
		(312)	1.611
10	1.549	(313)	1.555
		(230)	1.541
20	1.437	(040)	1.435
10	1.391	(234)	1.397

^aCalculated on the basis of a monoclinic unit cell with $a = 5.20$ Å, $b = 5.74$ Å, and $c = 13.28$ Å, $\beta = 90.2^\circ$, $Z = 4$; $V = 59.685$ cm³/mole.

TABLE II. X-ray-diffraction data of TiReO_4 (III) at 14.5 GPa and at room temperature.

I/I_0	$d_{\text{(obs)}}$	(hkl)	$d_{\text{(cal)}}$ ^a
5	3.636	(022)	3.650
50	3.359	(003)	3.352
100	3.196	(013)	3.196
100	3.120	($\bar{1}$ 22)	3.196
20	2.989	(130)	2.981
		(122)	2.978
20	2.770	(103)	2.781
		(200)	2.763
10	2.655	(040)	2.655
20	2.259	($\bar{1}$ 33)	2.270
		($\bar{2}$ 22)	2.259
20	2.190	(133)	2.187
		($\bar{1}$ 42)	2.187
		(114)	2.183
20	2.026	($\bar{2}$ 32)	2.040
		($\bar{2}$ 23)	2.039
		(213)	2.024
25	1.933	($\bar{2}$ 04)	1.928
		(223)	1.922
10	1.852	(241)	1.864
		(300)	1.842
10	1.805	(204)	1.798
		($\bar{2}$ 24)	1.812

^aCalculated on the basis of a monoclinic unit cell with $a = 5.54$ Å, $b = 10.62$ Å, and $c = 10.08$ Å, $\beta = 94^\circ$, $Z = 8$; $V = 44.541$ cm³/mole.

similar (Fig. 1), and further, the volume change at the transition is essentially zero (Fig. 3). We have therefore labeled the new phase that is stable between 1.0 and 1.85 GPa as phase (I'). The presence of a subtle phase transition near ~ 1.0 GPa is in accordance with the previous conclusion based on a high-pressure Raman study.³

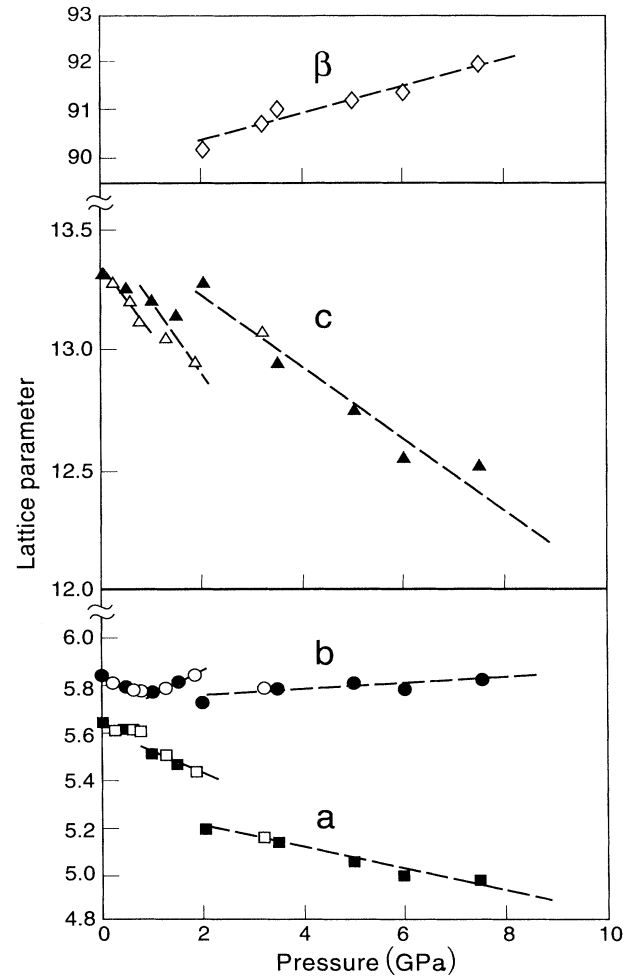


FIG. 2. Effect of pressure on the lattice parameters (a , b , c , and β) for TiReO_4 (I), (I'), and (II).

TABLE III. The effect of pressure on the lattice parameters and molar volume of TiReO_4 (I), TiReO_4 (I'), TiReO_4 (II), and TiReO_4 (III) phases. Note: The letters A and E indicate the angular-dispersive mode and the energy-dispersive mode, respectively.

Run Number	P (GPa)	a (Å)	b (Å)	c (Å)	β (deg)	V (cm ³ /mole)	V/V_0
A-0	0.001	5.631	5.840	13.314		65.916	1.000
E-1	0.25	5.615	5.820	13.29		65.385	0.992
A-1	0.50	5.620	5.814	13.26		65.228	0.990
E-2	0.60	5.617	5.80	13.20		64.742	0.982
E-3	0.75	5.610	5.79	13.12		64.159	0.974
A-2	1.00	5.51	5.78	13.20		63.229	0.960
E-4	1.30	5.50	5.80	13.05		62.673	0.951
A-3	1.50	5.46	5.82	13.15		62.910	0.954
E-5	1.85	5.43	5.86	12.95		62.037	0.941
A-4	2.00	5.20	5.74	13.28	90.2	59.685	0.905
E-6	3.20	5.18	5.80	13.08	90.7	59.168	0.898
A-5	3.5	5.15	5.80	12.95	91.0	58.236	0.883
A-6	5.00	5.05	5.85	12.75	91.2	56.704	0.860
A-7	6.00	5.01	5.81	12.55	91.4	54.990	0.834
A-8	7.5	4.98	5.84	12.53	92.0	54.838	0.831
A-9	10.5	5.80	10.62	10.15	92.0	47.041	0.714
A-10	14.5	5.54	10.62	10.08	94.0	44.541	0.676

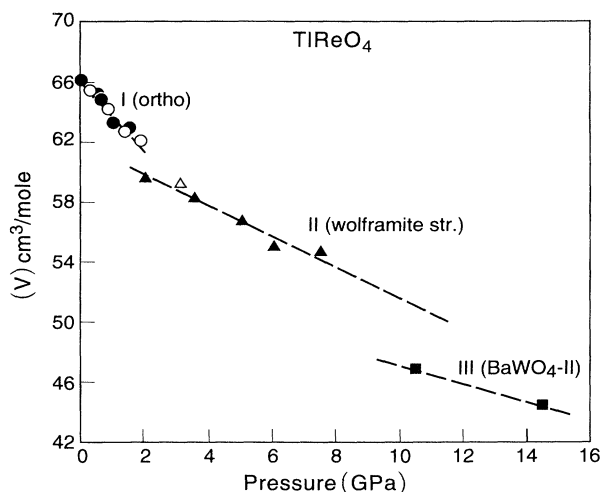


FIG. 3. Effect of pressure on the molar volumes of TiReO_4 (I), (I'), (II), and (III). The volume change at the transition between phases (I) and (I') is negligible, and about 2% and 9% at the two subsequent transitions.

TiReO_4 (II)

An important question that we next address is the structures of phase (II) and phase (III). Since both TiReO_4 (I) and (I') phases have the pseudoscheelite structure, it is reasonable to expect that TiReO_4 would assume the high-pressure structures encountered in other ABO_4 compounds with the scheelite or scheelite-related structures. We therefore, discuss below these possibilities, in the light of the existing high-pressure crystal chemistry of ABO_4 compounds.

In ABO_4 compounds, three high-pressure phases are encountered, which are all monoclinic, having a smaller volume with respect to their low-pressure counterpart. The most common one is the monoclinic wolframite-type structure in which many divalent tungstates with the smaller A cation (i.e., Mg, Mn, Fe, Co, Ni, Zn, and Cd) crystallize.⁶ Further, it has been reported that several AMoO_4 molybdates ($A = \text{Mg, Ni, Fe, Co, Mn, and Zn}$) have the wolframite-type structure when subjected to 6 GPa and 900 °C and quenched.⁷ Although a direct transformation of a scheelite-type compound to wolframite structure has not been observed so far in any ABO_4 tungstate or molybdate, crystal chemical considerations indicate that the molar volume change in the event of such a transition would be very small, as can be deduced from the example of the CdMoO_4 (scheelite) and the CdWO_4 (wolframite). The unit-cell volumes of CdMoO_4 and the CdWO_4 on a comparable basis are 297.3 and 298.7 Å³, respectively.⁶ It is well known that the volume difference between the tungstate and the molybdate of the same A cation is small.⁶ These facts suggest that the ΔV in the event of a scheelite to wolframite transformation in CdMoO_4 , for instance, would be very small. A different monoclinic phase has been reported in the case of PbWO_4 (II), a mineral called raspite assigned to the space group $P2_1/a$ or $P2_1/m$ with lattice parameters: $a = 13.525$ Å,

$b = 4.968$ Å, $c = 5.546$ Å, and $\beta = 107.75^\circ$. The molar volume of this phase is $\sim 0.8\%$ smaller than that of scheelite-type PbWO_4 (I).⁸ A third type of monoclinic phase is encountered in HgWO_4 and HgMoO_4 at ambient pressure, which is related to the wolframite type. The space group is $C2/c$ and the lattice parameters are $a = 13.525$ Å, $b = 4.968$ Å, $c = 5.546$ Å, and $\beta = 107.75^\circ$ for HgMoO_4 , and $a = 13.525$ Å, $b = 4.968$ Å, $c = 5.546$ Å, and $\beta = 107.75^\circ$ for HgWO_4 .⁹ In both structures, zig-zag chains of the edge-shared WO_6 or MoO_6 octahedra run along the c axis. In this phase of HgWO_4 and HgMoO_4 the oxygens form a nearly cubic close-packed array, in contrast to the ideal close packed array in the case of wolframite structure.⁹ Comparing our x-ray data given in Table I with the monoclinic phases described above, we find that the monoclinic phase (II) of TiReO_4 with lattice parameters $a = 5.20$ Å, $b = 5.74$ Å, $c = 13.28$ Å, and $\beta = 90.2^\circ$ is closest to the wolframite-type structure except for the doubling along the c axis, $c_{\text{II}} \sim 2c_w$ (e.g., $a = 5.029$ Å, $b = 5.859$ Å, $c = 5.074$ Å, and $\beta = 91.47^\circ$ in the case of CdWO_4).⁶ Without this doubling the two d spacings observed in the diffraction patterns of TiReO_4 (II) at 3.673 Å and 1.391 Å do not fit, although the Miller indices assigned to the rest of the diffraction lines in phase (II) fall in line with the wolframite structure. Hence we believe that phase (II) is a superstructure of the normal wolframite type. However, on examining closely the x-ray-diffraction patterns at pressures between 2 and 7.5 GPa (see Fig. 1), we observe additional lines corresponding to (hkl) of (203), (013), (004), and (023) developing in the range of 3.2 to 5.0 GPa. This seems to indicate that the phase transition takes place over a range of pressure, starting from 2.0 to 5.0 GPa. The volume change ΔV of $\sim 2\%$ would be reasonable in view of the fact that the orthorhombic pseudoscheelite phase (I) of TiReO_4 is 1.85% larger in molar volume compared to the normal scheelite phase of TiReO_4 .¹ Therefore, we conclude that the phase transition observed at 2 GPa in TiReO_4 is basically from scheelite to wolframite type, which was also suggested in the earlier Raman study by Jayaraman, Kourouklis, and Van Uitert.

Nicol and Durana¹⁰ proposed a transition from the scheelite to wolframite structure in CaMoO_4 and CaWO_4 , at ~ 2.7 and ~ 1.2 GPa, respectively, from their high-pressure Raman studies. However, their Raman evidence was not confirmed in subsequent high-pressure Raman studies.^{11,12} Our most recent high-pressure Raman studies (to be published) on CdMoO_4 have shown that a pressure-induced scheelite to wolframite transition occurs in this material near 12 GPa. This would be a very good example to study by high-pressure x-ray diffraction, to actually prove some of our statements made earlier in this section.

TiReO_4 (III)

Our results are consistent with the monoclinic lattice for phase (III). The most likely structure analog for this phase would be the BaWO_4 (II) type, which was synthesized by subjecting the scheelite-type BaWO_4 to 4–6

GPa at temperatures in the range of 600–1000 °C followed by quenching.^{13,14} The quenched phase is ~12% denser than the scheelite-type BaWO₄.¹³ The large density increase in BaWO₄ (II) appears to be mainly due to a densely packed two-dimensional network of WO₆ octahedra, with Ba cations in either eight-coordinated or nine-coordinated sites.¹⁴ A high-pressure phase isostructural to BaWO₄ (II) has also been reported in the case of PbWO₄.¹⁵

Fukunaga and Yamaoka¹⁶ have suggested a graphic method to predict the high-pressure structures of ABO₄-type compounds. In this method, they plot the parameter $t = (r_A + r_B) / 2r_O$ against $k = r_A / r_B$ for numerous ABO₄ compounds crystallizing in different structures, where r_A , r_B , and r_O are ionic radii of *A* and *B* cations and the divalent oxygen, respectively. According to them, pressure generally favors a phase with a larger value of *t* in the *t*-*k* diagram. From this criterion they have suggested that ABO₄ compounds with either the scheelite or the wolframite structure would eventually transform to the BaWO₄ (II) structure.

Comparing our x-ray-diffraction data of phase (III) with that of BaWO₄ (II), we find two important features: (1) closely related lattice parameters such that $a(\text{III}) \sim \frac{1}{2}a_0(\text{BaWO}_4\text{-II})$, $b(\text{III}) \sim \sqrt{2}b_0(\text{BaWO}_4\text{-II})$, $c(\text{III}) \sim \sqrt{2}c_0(\text{BaWO}_4\text{-II})$, and $\beta(\text{III}) \sim \beta(\text{BaWO}_4\text{-II})$, and (2) comparable ΔV_0 of the transition (as can be seen in the next section, the volume difference at the ambient pressure between phase (I) and phase (III) of TiReO₄ is ~10%, as against ΔV_0 of 12% between phase (I) and phase (II) of BaWO₄). From these considerations, we believe that the monoclinic phase (III) of TiReO₄ is quite similar to the monoclinic BaWO₄ (III). However, it should be noted that while the monoclinic BaWO₄ (II) can be quenched from high pressures, the monoclinic TiReO₄ (III) is not quenchable and reverts back to its low-pressure form when pressure is released.

Isothermal compression of TiReO₄

Assuming a linear relationship, the axial compressibility along *a*, *b*, and *c* was calculated for phases (I), (I'), and (II). This was not possible for the phase (III) for paucity of data points. The values are listed in Table IV. It is of interest to note (1) that the anisotropic feature is common to all the three phases, with the most compressible direction being the *c* axis, (2) that although the phases (I') and phase (II) have a similar unit cell, their linear compressibilities are very different from each other, and (3) that al-

TABLE IV. Linear compressibilities (in GPa⁻¹) of TiReO₄ (I), TiReO₄ (I'), and TiReO₄ (II).

Phase	<i>a</i>	<i>b</i>	<i>c</i>
(I)	4.3×10^{-3}	11.0×10^{-3}	18.0×10^{-3}
(I')	18.0×10^{-3}	-17.0×10^{-3}	19.0×10^{-3}
(II)	8.5×10^{-3}	-2.6×10^{-3}	10.7×10^{-3}

TABLE V. Zero-pressure bulk modulus (K_0 in GPa) and molar volume (V_0 in cm³/mole) for ABO₄ compounds with scheelite or scheelite-related structure.

Compounds	V_0	K_0	Ref.
TiReO ₄ ^a	65.916	26	This study
CaWO ₄	47.07	68	17
CaMoO ₄	46.90	81	17
		85	12
CdMoO ₄	44.77	104	17
PbMoO ₄	53.85	64	17
PbWO ₄	54.05	64	17
SrMoO ₄	52.6	73	18
BiVO ₄ ^a	45.9	150	19
LaNbO ₄ ^a	50.11	111	20

^aDistorted scheelite structure.

though the linear compressibility β_a and β_c for phases (I') and (II) are quite similar, the β_b is negative, indicating that the *b* axis expands upon compression.

The bulk modulus K_0 and its pressure derivative K'_0 can be calculated by fitting the *P*-*V* data to the second-order Birch-Murnaghan equation:

$$P = 1.5K_0[X^{(-7/3)} - X^{(-5/3)}][1 - \xi(X^{(-2/3)} - 1)], \quad (1)$$

where $X = V/V_0$, $\xi = 0.75(4 - K'_0)$ and $K'_0 = (dK_0/dP)T$.

Practically no volume change is involved between phases (I) and (I'), and hence we fit the *P*-*V* data from 0 to 1.85 GPa. Assuming $K'_0 = 4$, the value of K_0 for phase (I) and (I') is determined as 26 GPa. For comparison, we have collected in Table V the available data of bulk modulus for compounds with scheelite and scheelite-related structures. It is evident that the bulk modulus derived for TiReO₄ is the lowest. By comparing the relative compressibility of scheelite-type compounds, Hazen, Finger, and Mariathan¹⁷ have found that the compressibility in these compounds is mainly governed by the compressibility of the eightfold-coordinated *A* cation polyhedra, which in turn is proportional to the polyhedral volume divided by the cation formal charge. It was therefore suggested that the most compressible scheelite compounds would be $A^{+1}B^{+7}O_4$ (CsReO₄ and RbRuO₄), followed by $A^{+2}B^{+6}O_4$ such as alkaline-earth molybdates and tungstates, which are significantly less compressible. The ABO₄ compounds with cations A^{+3} and B^{+5} (e.g., LaNbO₄) are expected to be even less compressible, the least compressible ones being $A^{+4}B^{+4}O_4$, viz. ZrGeO₄ and the high-pressure phase of ZrSiO₄. On the basis of the data given in Table V, we have plotted in Fig. 4 $\ln K_0$ against $\ln V_0$ for ABO₄ compounds with scheelite and the scheelite-related structure. It is evident that there are two well-defined K_0 - V_0 systematics for the $A^{+2}B^{+6}O_4$ molybdates, and the $A^{+3}B^{+5}O_4$ compounds, respectively, thus providing strong support for the suggestion made by Hazen, Finger, and Mariathan.¹⁷ We therefore believe that TiReO₄ should be grouped along with alkali perhenates such as KReO₄, CsReO₄, and RbRuO₄ and form a similar systematics below that of molybdates as indicated by the

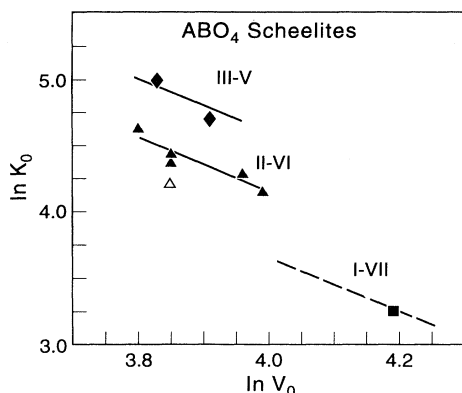


FIG. 4. The bulk modulus-volume systematics for the ABO_4 compounds with scheelite or scheelite-related structure based on the data given in Table V, where \blacktriangle and \triangle stand for molybdates and calcium tungstate, respectively; \blacklozenge for III-V compounds and \blacksquare for $TlReO_4$ of this study.

subparallel dashed-line through the $TlReO_4$ data point in Fig. 4.

To calculate the bulk modulus of phase (II), we had to adopt the method suggested for high-pressure phases, based on finite-strain analysis.²¹ To carry out this, the pressure and volume data are first converted into a normalized pressure (G) and a strain parameter (g) such that

$$G = P / [3(1 + 2g)^{2.5}],$$

and

$$g = 0.5[(V_{02}/V_{01})^{-2/3} - 1]. \quad (2)$$

Then the converted data of G and g are fitted to the finite-strain expansion of the stress G such that

$$G = a + bg + cg^2 + dg^3 + \dots \quad (3)$$

The coefficients of a , b , c have been derived as

$$a = [(\alpha^2 - 1)/2]\alpha^5 K_{02} [1 + \xi(1 - \alpha^2)], \quad (4)$$

$$b = \alpha^7 K_{02} [1 + 2(1 - \alpha^2)], \quad (5)$$

$$c = -2\alpha^9 K_{02}, \quad (6)$$

where $\alpha = (V_{01}/V_{02})^{1/3}$, and $\xi = 0.75(4 - K'_{02})$. Value of K_{02} and K'_{02} can be determined from the fitted coefficients a , b , and c , using equations given above.

Because of the scatter in the x-ray-diffraction data coupled with the limited pressure range over which they were available for the high-pressure phases (II) and (III), a simultaneous fit of K_0 and K' was not physically realistic. Therefore a linear fit was attempted. On the basis of the intercept a and the slope b (see Fig. 5), the V_{02}/V_{01} and K_{02} are calculated for phase (II) to be 0.94 and 45.6 GPa. Similar calculations for the phase (III) yield V_{03}/V_{01} and K_{03} at 0.90 and 47.6 GPa, respectively. These results are in accord with the general rule that the bulk modulus of high-pressure phases should be higher than that of the low-pressure phases.

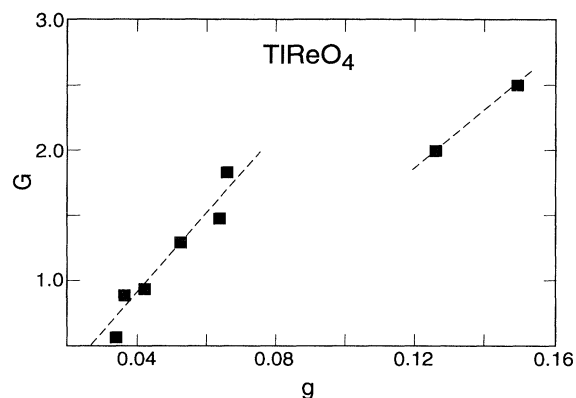


FIG. 5. The relationship between the normalized strain (g) and the normalized stress (G) for the $TlReO_4$ (II) and (III). Data for phase (II) and phase (III) can be represented by linear lines: $G = -0.45 + 32.61g$, and $G = -0.84 + 22.4g$, respectively. The zero-pressure volume (V_0) and the bulk modulus (K_0) of each high-pressure phase can then be calculated from the intercept and the slope of the fitted line as described in the text.

IV. SUMMARY AND CONCLUSIONS

Our high-pressure x-ray studies confirm the three pressure-induced phase transformations reported in $TlReO_4$ from a high-pressure Raman study. Analysis of the x-ray data have led to the identification of the three high-pressure phases as orthorhombic (I'), monoclinic wolframite related phase (II) and yet another monoclinic $BaWO_4$ (II) related phase. From arguments based on high-pressure crystal chemistry of the ABO_4 compounds and the volume changes ΔV at the transitions, the above identifications are justified.

We believe that a single-crystal high-pressure x-ray-diffraction study on $TlReO_4$ is possible since the small volume changes at the first two transitions probably would not rupture the crystal. Further, the transition pressures are below 2 GPa, well within the capability of the Merrill-Bassett cell. Such a study would enable detailed and precise information regarding the structure of the high-pressure phases (I') and (II). It may be possible to obtain richer powder x-ray-diffraction data on phase (III) using synchrotron radiation, and to elucidate further the structural aspects of the phase.

Thallium perrhenate is a remarkable material with an electronic transition near 10 GPa involving charge transfer from Tl to Re. Pushing the system into the metallic state below a megabar pressure is a very good possibility. Phase (I') should be investigated for possible ferro-antiferro electric properties, as well as ferroelastic behavior.

ACKNOWLEDGMENTS

Work was done partially at SSRL which is operated by the Department of Energy, Office of Basic Energy Sci-

ences. We thank J. Balogh for setting up the remotely controlled collimator system and for his assistance in many aspects during the experiments. We are also grateful for J. Park for her assistance in the data collection at

SSRL. This work was partially supported by a NSF grant (DMR94-0-2443). One of us (Y.H.K.) would like to thank the Pohang Light Source Laboratory (PLS) of Korea for a travel grant (PLS 94-07).

-
- ¹A. Jayaraman, A. Kourouklis, R. M. Fleming, and L. G. Van Uitert, *Phys. Rev. B* **37**, 664 (1988).
²A. Jayaraman, A. Kourouklis, and L. G. Van Uitert, *Phys. Rev. B* **36**, 8547 (1987).
³L. C. Ming, A. Jayaraman, S. R. Shieh, Y. H. Kim, and M. H. Manghnani, *J. Phys. Chem. Solids* **55**, 1207 (1994).
⁴L. C. Ming and M. H. Manghnani, *J. Appl. Phys.* **49**, 208 (1978).
⁵D. L. Decker, *J. Appl. Phys.* **42**, 3239 (1971).
⁶A. W. Sleight, *Acta Crystallogr. B* **28**, 2899 (1972).
⁷A. P. Young and C. M. Schwartz, *Science* **141**, 348 (1963).
⁸R. Shaw and G. F. Claringbull, *Am. Mineral* **40**, 933 (1955).
⁹W. Jeitschko and A. W. Sleight, *Acta Crystallogr. B* **29**, 869 (1973).
¹⁰M. Nicol and J. F. Durana, *J. Chem. Phys.* **54**(4), 1436 (1971).
¹¹A. Jayaraman, B. Batlogg, and L. G. Van Uitert, *Phys. Rev. B* **28**, 4774 (1983).
¹²D. Christofilos, A. Kourouklis, and S. Ves, *J. Phys. Chem. Solids* (to be published).
¹³T. Fujita, S. Yamaoka, and O. Fukunaga, *Mater. Res. Bull.* **9**, 141 (1974).
¹⁴I. Kawada, K. Kato, and T. Fujita, *Acta Crystallogr. B* **30**, 2069 (1974).
¹⁵P. W. Richter, G. J. Kruger, and C. W. F. T. Pistorius, *Acta Crystallogr. B* **32**, 928 (1976).
¹⁶O. Fukunaga and S. Yamaoka, *Phys. Chem. Miner.* **5**, 167 (1979).
¹⁷R. M. Hazen, L. W. Finger, and J. W. E. Mariathasan, *J. Phys. Chem. Solids* **46**, 253 (1985).
¹⁸R. F. S. Hearmon, in *Numerical Data and Functional Relationship in Sciences and Technology*, edited by K-H. Hellwege and A. M. Hellwege, Landolt-Börnstein, New Series, Group III, Vol. 11, p. 61 (Springer-Verlag, Berlin, 1979).
¹⁹R. M. Hazen and J. W. E. Mariathasan, *Science* **216**, 991 (1982).
²⁰J. W. E. Mariathasan, L. W. Finger, and R. M. Hazen, *Acta Crystallogr. B* **41**, 179 (1985).
²¹R. Jeanloz, *Geophys. Res. Lett.* **8**, 1219 (1981).